Chemical functionality of Multidomain Peptide Hydrogels governs early host immune response

Tania L. Lopez-Silva[a], David G. Leach[a], Alon Azares[c], I-Che Li[a], Darren G. Woodside[c], Jeffrey D. Hartgerink[a,b,]*

[a] *Department of Chemistry, Rice University, Houston, Texas 77005, USA*
[b] *Department of Bioengineering, Rice University, Houston, Texas 77005, USA*
[c] *Department of Molecular Cardiology, Texas Heart Institute, Houston, Texas, 77030, USA*

Corresponding Author
*Email: jdh@rice.edu

Supporting Information

Table of contents

Table S1. Self-assembling Multidomain Peptides: peptide sequences and properties. **3**

Figure S1. MALDI TOF MS spectra of the diverse multidomain peptides: K_2, R_2, E_2, D_2. **4**

Figure S2. Viscoelastic properties of K_2, R_2, E_2, D_2 **5**

Table S2. Peptide sequence and viscoelastic properties of Multidomain Peptides **6**

Figure S3. Subcutaneous injection model **6**

Table S3. Immunophenotyping antibodies used for the flow cytometry panels. **7**

Table S4. Flow cytometry parameters and configuration for all studied panels. **8**

Figure S4. Gating strategy and t-SNE clustering method for flow cytometry data analysis **9**

Figure S5. H&E staining of the implant edge of K_2. R_2, E_2, D_2 at day 3, 7 and 10 post-injection **10**

Figure S6. H&E staining of the implant core of K_2. R_2, E_2, D_2 at day 3, 7 and 10 post-injection. **10**

Figure S7. H&E staining of the whole implant of K_2. R_2, E_2, D_2 at day 3 post-injection. **11**

Figure S8. H&E staining of the whole implant of K_2. R_2, E_2, D_2 at day 10 post-injection. **12**

Figure S9. Cell density present in the MDP implants at different time points. **13**

Figure S10. Collagen deposition and tissue remodeling of MDP hydrogel implants. **13**

Figure S11. Masson's Trichrome staining of K_2. R_2, E_2, D_2 at day 3 post-injection. **14**

Figure S12. Masson's Trichrome staining of K_2. R_2, E_2, D_2 at day 7 post-injection. **15**

Figure S13. Masson's Trichrome staining of K_2. R_2, E_2, D_2 at day 10 post-injection. **16**

Figure S14. Immunostaining of alpha-smooth-muscle actin **17**

Figure S15. Immunostaining of alpha-smooth-muscle actin K_2. R_2, E_2, D_2 at day 3 post-injection. **18**

Figure S16. Immunostaining of alpha-smooth-muscle actin of K_2. R_2, E_2, D_2 at day 7 post-injection **19**

Figure S17. Immunostaining of alpha-smooth-muscle actin of K_2. R_2, E_2, D_2 at day 10 post-injection. **20**

Figure S18. Gating strategy for the immunophenotyping of myeloid cells in the MDP hydrogels. **21**

Figure S19. Gating strategy for the immunophenotyping of lymphoid cells in the MDP hydrogels. **22**

Figure S20. Immunophenotyping of infiltrating cells in E_2 implants at day 3. **23**

Figure S21. Percentage of different lymphoid cell phenotypes from $CD45^+$ cells present in K_2 implants at day 1, 3, 7 and 10 post-injection. **24**

Figure S22. Quantification of IL-4 and INF-γ from the implant lysate. **24**

Figure S23. Gating strategy for the immunophenotyping of stem cells in the MDP hydrogels. **25**

Table S1. Self-assembling Multidomain Peptides: peptide sequences and properties.

Name	Sequence	Monoisotopic mass (Da)	Molecular weight (Da)	Molar concentration of 1wt. % solution
K_2	Ac-KKSLSLSLSLSLSLKK-$CONH_2$	1772.103	1773.171	5.6 mM
E_2	Ac-EESLSLSLSLSLSLEE-$CONH_2$	1775.893	1776.937	5.6 mM
R_2	Ac-RRSLSLSLSLSLSLRR-$CONH_2$	1885.225	1884.127	5.3 mM
D_2	Ac-DDSLSLSLSLSLSLDD-$CONH_2$	1720.829	1719.83	5.8 mM

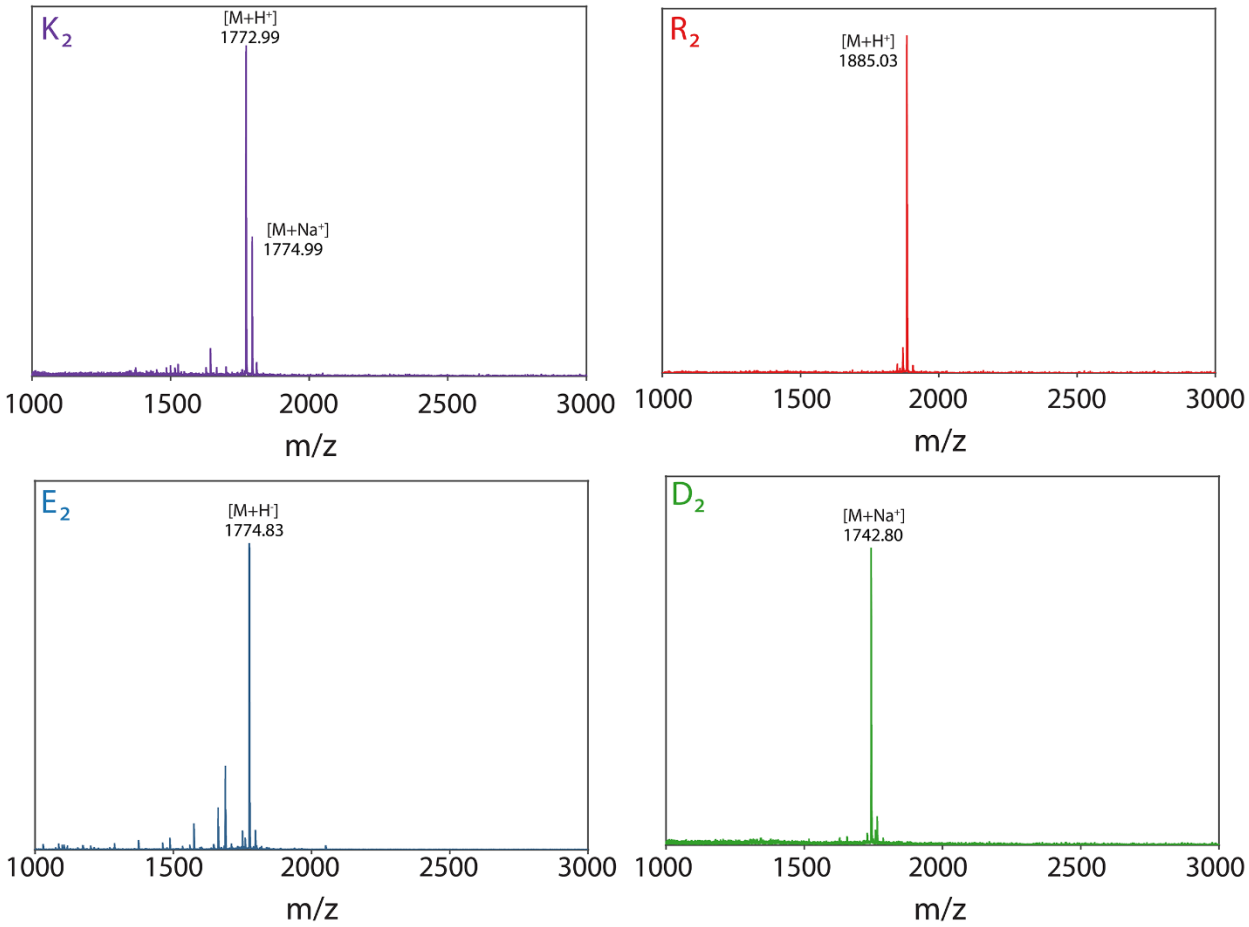

Figure S1. MALDI TOF MS spectra of the diverse multidomain peptides: K_2, R_2, E_2, D_2.

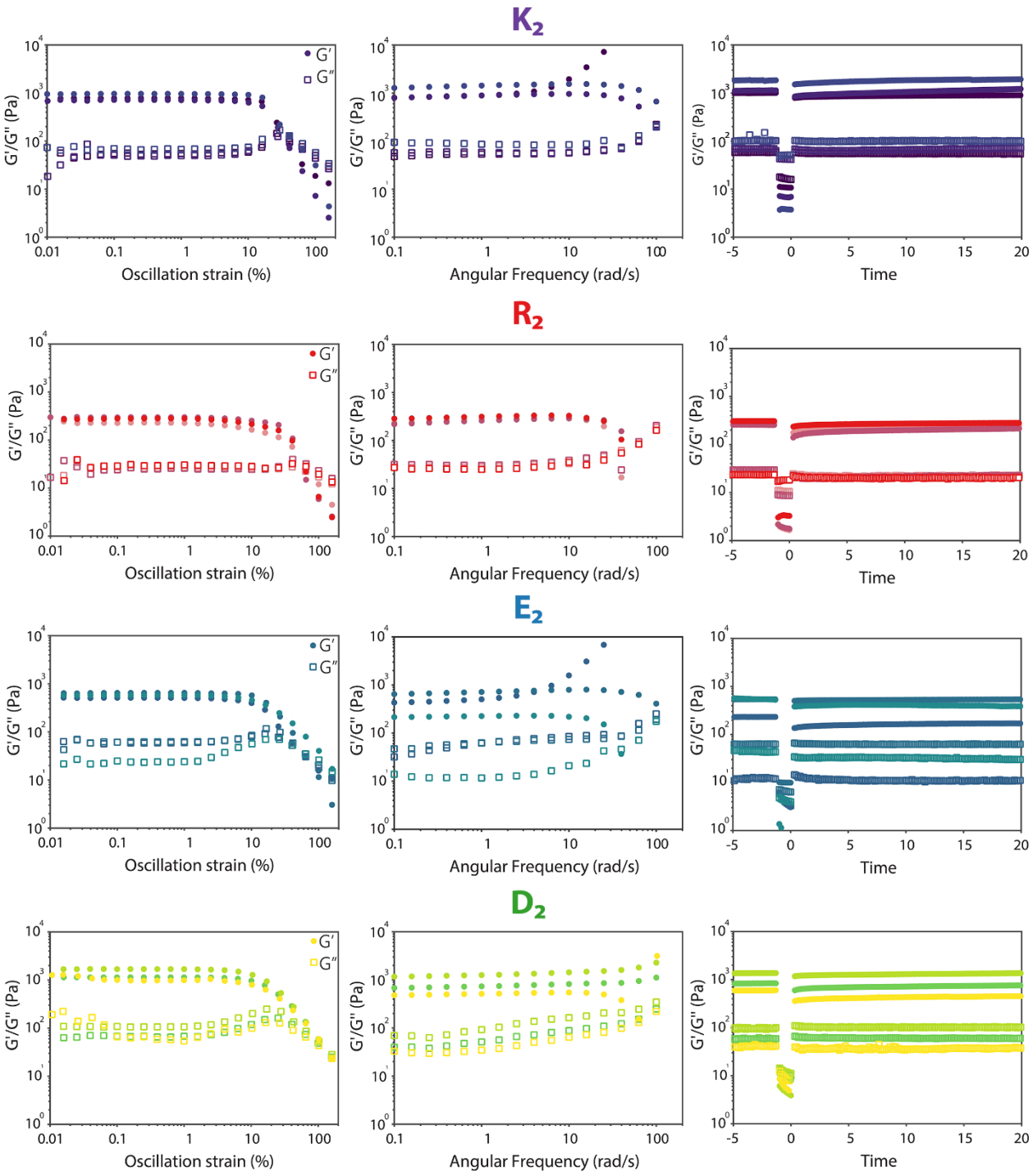

Figure S2. Viscoelastic properties of K_2, R_2, E_2, D_2 at 1% by weight in 149 mM sucrose 0.5X HBSS (amplitude sweep, frequency sweep and strain recovery). b) Storage and loss moduli of MDPs at 1% oscillatory strain. Peptide materials were analyzed in triplicate, all experimental results are shown in each plot.

Table S2. Peptide sequence and viscoelastic properties of Multidomain Peptides with different ionic domains. All peptides at 1% by weight in buffer form hydrogels that recover their viscoelastic properties after a shearing process.

Peptide	Sequence	G' (Pa)	G'' (Pa)	Shear Recovery (%)	
				1 min	20 min
K_2	Ac-KKSLSLSLSLSLSLKK-$CONH_2$	819 ± 131	57 ± 9	82 ± 4	100 ± 9
R_2	Ac-RRSLSLSLSLSLSLRR-$CONH_2$	269 ± 37	28 ± 2	71 ± 9	87 ± 4
E_2	Ac-EESLSLSLSLSLSLEE-$CONH_2$	579 ± 70	49 ± 22	77 ± 16	82 ± 15
D_2	Ac-DDSLSLSLSLSLSLDD-$CONH_2$	1271 ± 365	76 ± 27	81 ± 13	88 ± 12

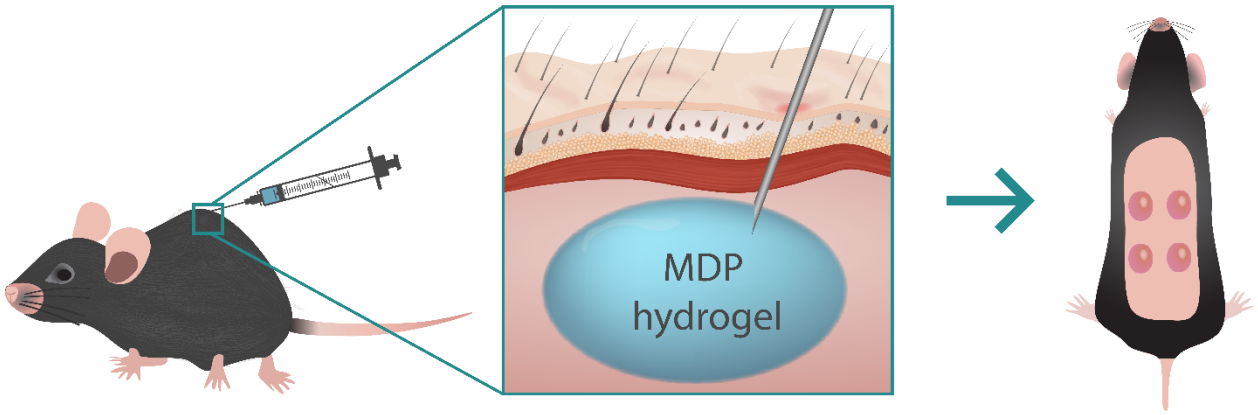

Figure S3. Subcutaneous injection model to evaluate the early host immune response to MDP hydrogels. Four injections of MDP hydrogel were distributed along the dorsal subcutaneous space.

Table S3. Immunophenotyping antibodies used for the flow cytometry panels.

Antibody	Clone	Isotype	Conjugate	Company	Catalog #
		Myeloid Panel			
CD45	30-F11	Rat IgG_{2b}, κ	APC-Cy7	BD Biosciences	561037
Gr-1	RB6-8C5	Rat IgG_{2b}, κ	APC	BD Biosciences	561083
Ly-6C	AL-21	Rat IgM, κ	PE-Cy7	BD Biosciences	560593
CD11b	M1/70	Rat IgG_{2b}, κ	FITC	BD Biosciences	561688
F4/80	T45-2342	Rat IgG_{2a}, κ	BV421	BD Biosciences	565411
		Lymphoid Panel			
CD45	30-F11	Rat IgG_{2b}, κ	APC-Cy7	BD Biosciences	561037
NK-1.1	PK136	Mouse IgG_{2a}, κ	PE	BD Biosciences	561046
CD11b	M1/70	Rat IgG_{2b}, κ	FITC	BD Biosciences	561688
CD3e	145-2C11	Armenian Hamster IgG_1, κ	BV510	BD Biosciences	563024
CD8a	53-6.7	Rat IgG_{2a}, κ	BV711	BD Biosciences	563046
CD4	GK1.5	Rat IgG_{2b}, κ	BUV395	BD Biosciences	563790
CD19	1D3	Rat IgG_{2a}, κ	BUV737	BD Biosciences	BUV737
		Stem Cell Panel			
CD45	30-F11	Rat IgG_{2b}, κ	APC-Cy7	BD Biosciences	561037
CD105	MJ7/18	Rat IgG_{2a}, κ	Alexa Fluor 647	BD Biosciences	562761
Ly6A-E (Sca-1)	E13-161.7	Ray IgG_{2a}, κ	PE	BD Biosciences	553336
CD38	90/CD38	Rat IgG_{2a}, κ	PerCP-Cy5.5	BD Biosciences	562770
CD11b	M1/70	Rat IgG_{2b}, κ	FITC	BD Biosciences	561688
CD29	Ha2/5	Hamster IgM, κ	BV421	BD Biosciences	564131
CD117	2B8	Rat IgG_{2b}, κ	BUV395	BD Biosciences	564011
		Isotype Controls and other			
Rat IgG_{2b}, κ	A95-1		FITC	BD Biosciences	553988
Rat IgM, κ	R4-22		PE-Cy7	BD Biosciences	560572
Rat IgG_{2a}, κ	R35-95		BV421	BD Biosciences	562602
Mouse IgG_{2a}, κ	G155-178		PE	BD Biosciences	553457
Rat IgG_{2a}, κ	R35-95		BUV737	BD Biosciences	564294
Rat IgG_{2b}, κ	A95-1		APC-Cy7	BD Biosciences	552773
Rat IgG_{2b}, κ	A95-1		APC	BD Biosciences	553991
Hamster IgG_1, κ	A19-3		BV510	BD Biosciences	563197
Rat IgG_{2a}, κ	R35-95		BV711	BD Biosciences	563047
Rat IgG_{2b}, κ	R35-38		BUV395	BD Biosciences	563560
Blue live/dead				Invitrogen	L38961

Table S4. Flow cytometry parameters and configuration for all studied panels.

Myeloid Panel

Laser	Marker	Fluorophore	Filter
Red (633 nm)	CD45	APC-Cy7	780/60
	Gr-1 (Ly6C & Ly6G)	APC	660/20
Y&G (561 nm)	Ly-6C	PE-Cy7	780/60
Blue (488 nm)	CD11b	FITC	530/30
Violet (407 nm)	F4/80	BV421	450/50
UV (355 nm)	Live/dead Blue		450/50

Lymphoid Panel

Laser	Marker	Fluorophore	Filter
Red (633 nm)	CD45	APC-Cy7	780/60
Y&G (561 nm)	NK-1.1	PE	585/15
Blue (488 nm)	CD11b	FITC	530/30
Violet (407 nm)	CD3e	BV510	525/50
	CD8a	BV711	710/50
UV (355 nm)	CD4	BUV395	379/28
	CD19	BUV737	740/35
	Live/dead Blue		450/50

Stem Cell Panel

Laser	Marker	Fluorophore	Filter
Red (633 nm)	CD45	APC-Cy7	780/60
	CD105	Alexa Fluor 647	660/20
Y&G (561 nm)	Ly6A-E	PE	585/15
	CD38	PerCP-Cy5.5	695/40
Blue (488 nm)	CD11b	FITC	530/30
Violet (407 nm)	CD29	BV421	450/50
UV (355 nm)	CD117	BUV395	379/28
	Live/dead		450/50

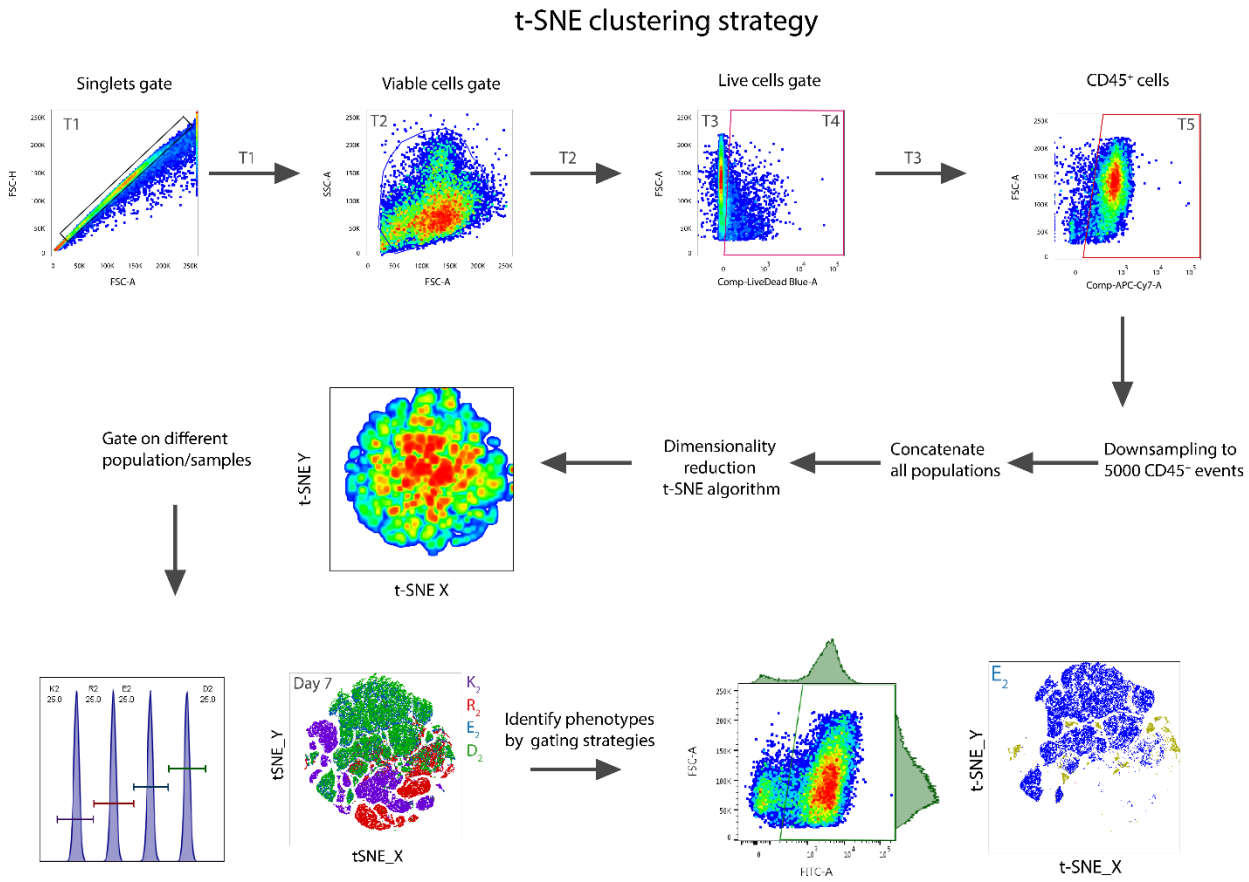

Figure S4. Gating strategy and t-SNE clustering method for flow cytometry data analysis. Singles cells were gated from FSC-H vs FSC-A, followed by viable cells discrimination. Then live/dead gating was used to take live cells only and from them CD45+ immune cells were gated. All samples from each peptide or timepoint were downsampled to 5000 CD45 positive events and concatenated in a single FCS file. Dimensionality reduction by the t-SNE algorithm was performed using FlowJo v10 with the following parameters: 1000 iteration, perplexity value 30, eta value 200 and theta of 0.5. Clusters were gated according to the peptide or timepoint as well as phenotype using the myeloid strategy shown in Figure S18.

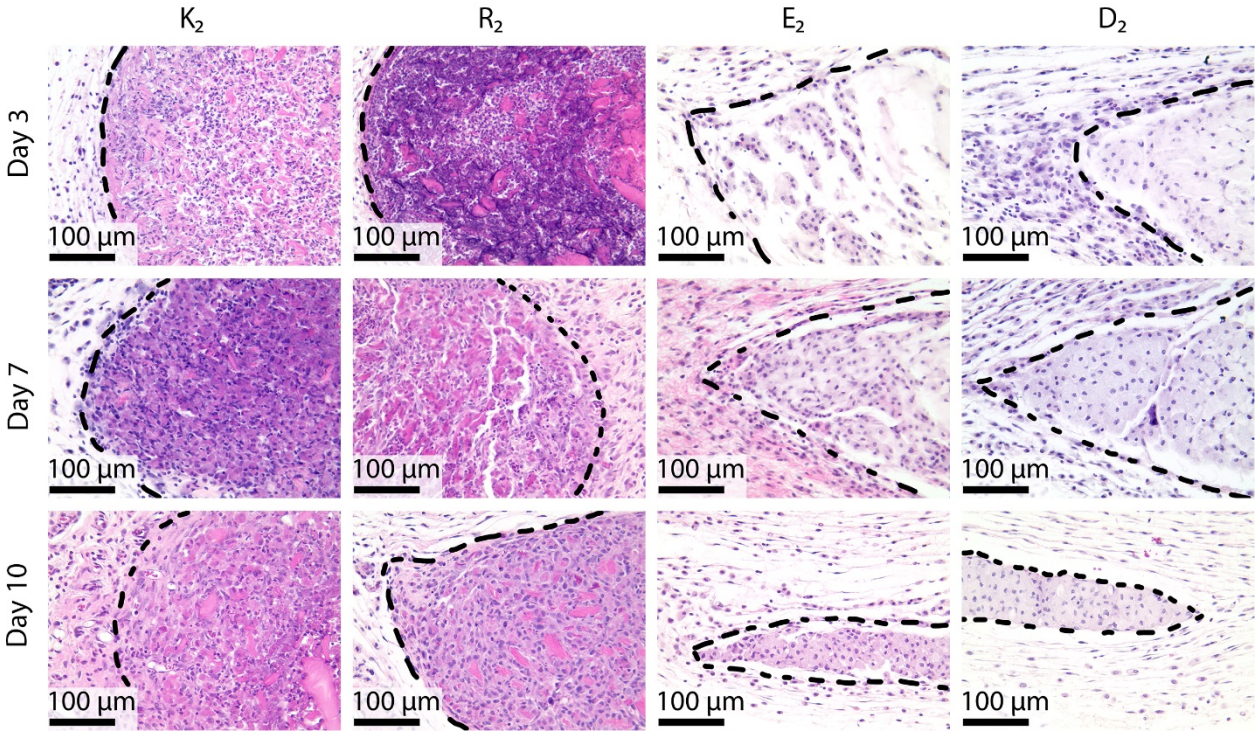

Figure S5. H&E staining of the implant edge of K_2. R_2, E_2, D_2 at day 3, 7 and 10 post-injection. Scale bar: 100 μm.

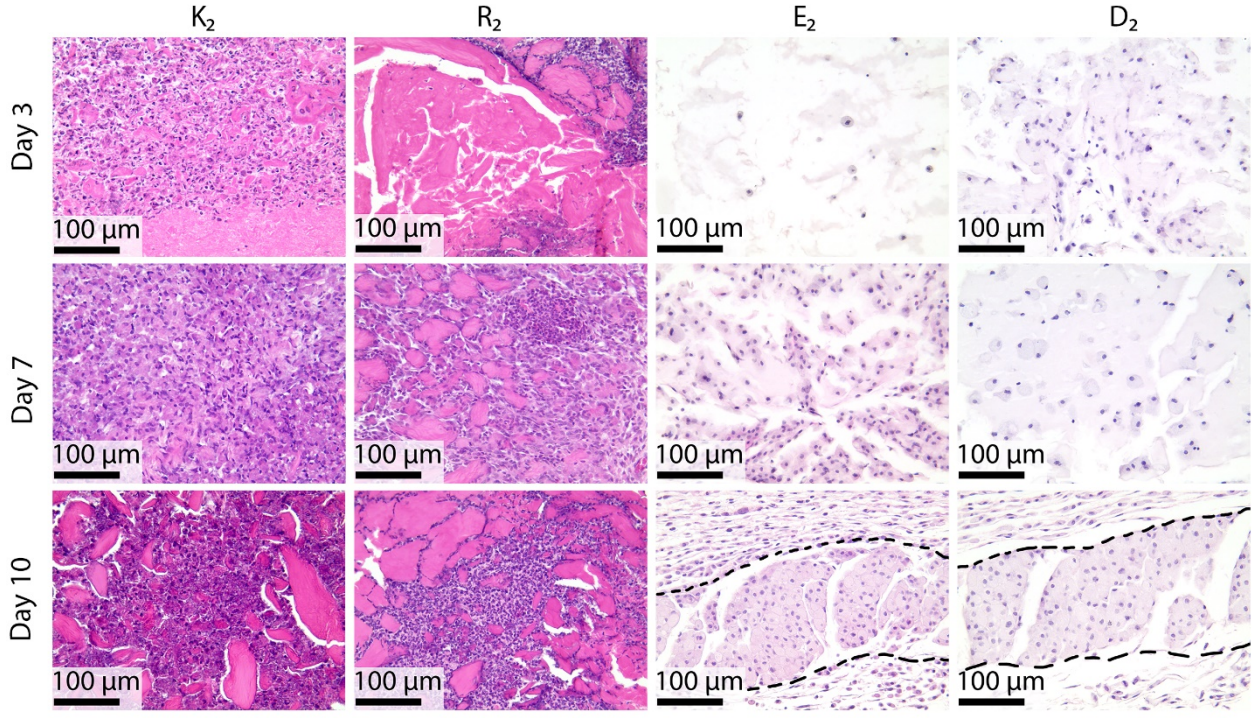

Figure S6. H&E staining of the implant core of K_2. R_2, E_2, D_2 at day 3, 7 and 10 post-injection. Scale bar: 100 μm.

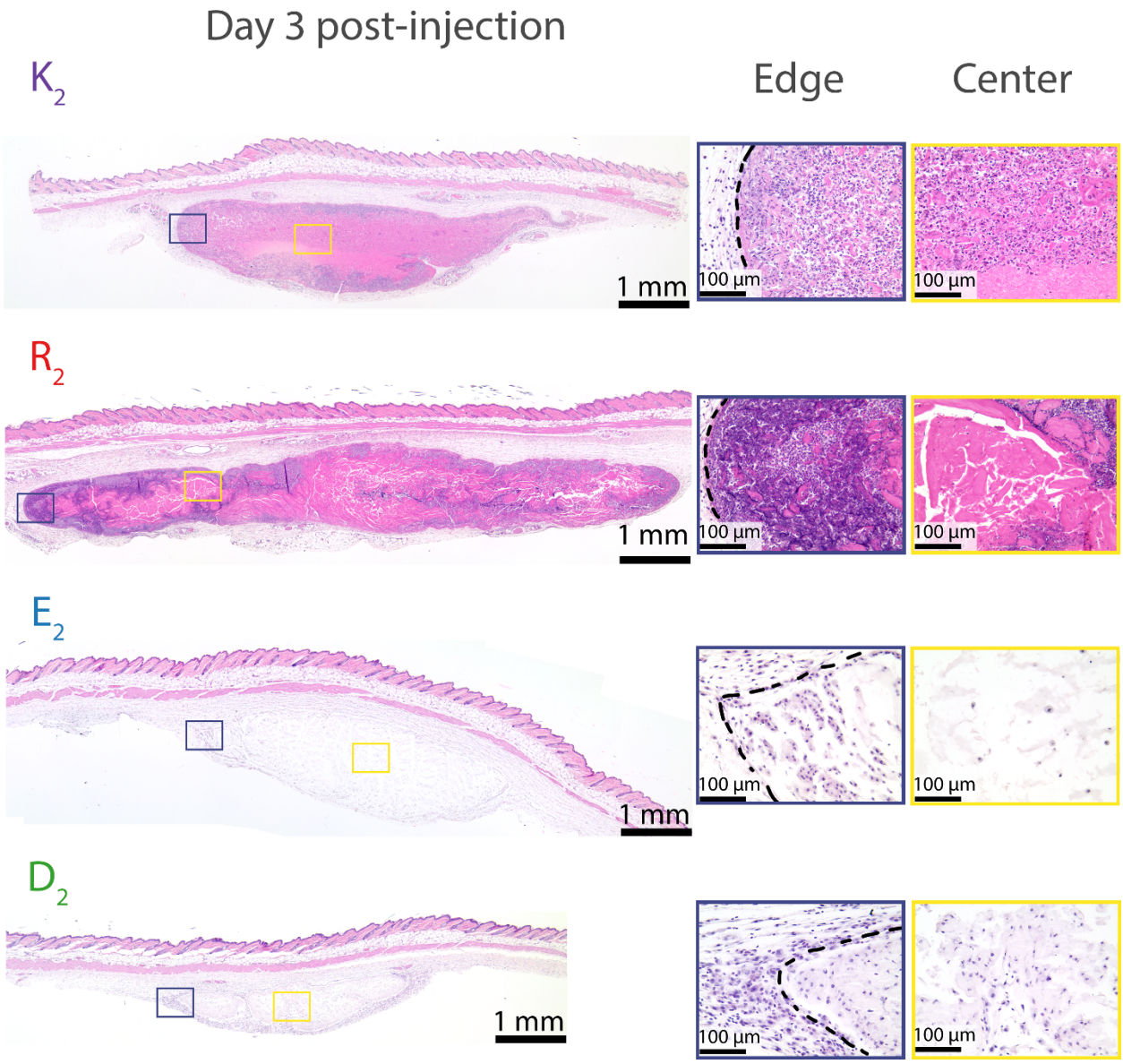

Figure S7. H&E staining of the whole implant of K_2. R_2, E_2, D_2 at day 3 post-injection. the purple box represents the area of the implant edge. The yellow box represents the area of the implant center. Dash lines represent the hydrogel in the subcutaneous space. Scale bar: 1 mm.

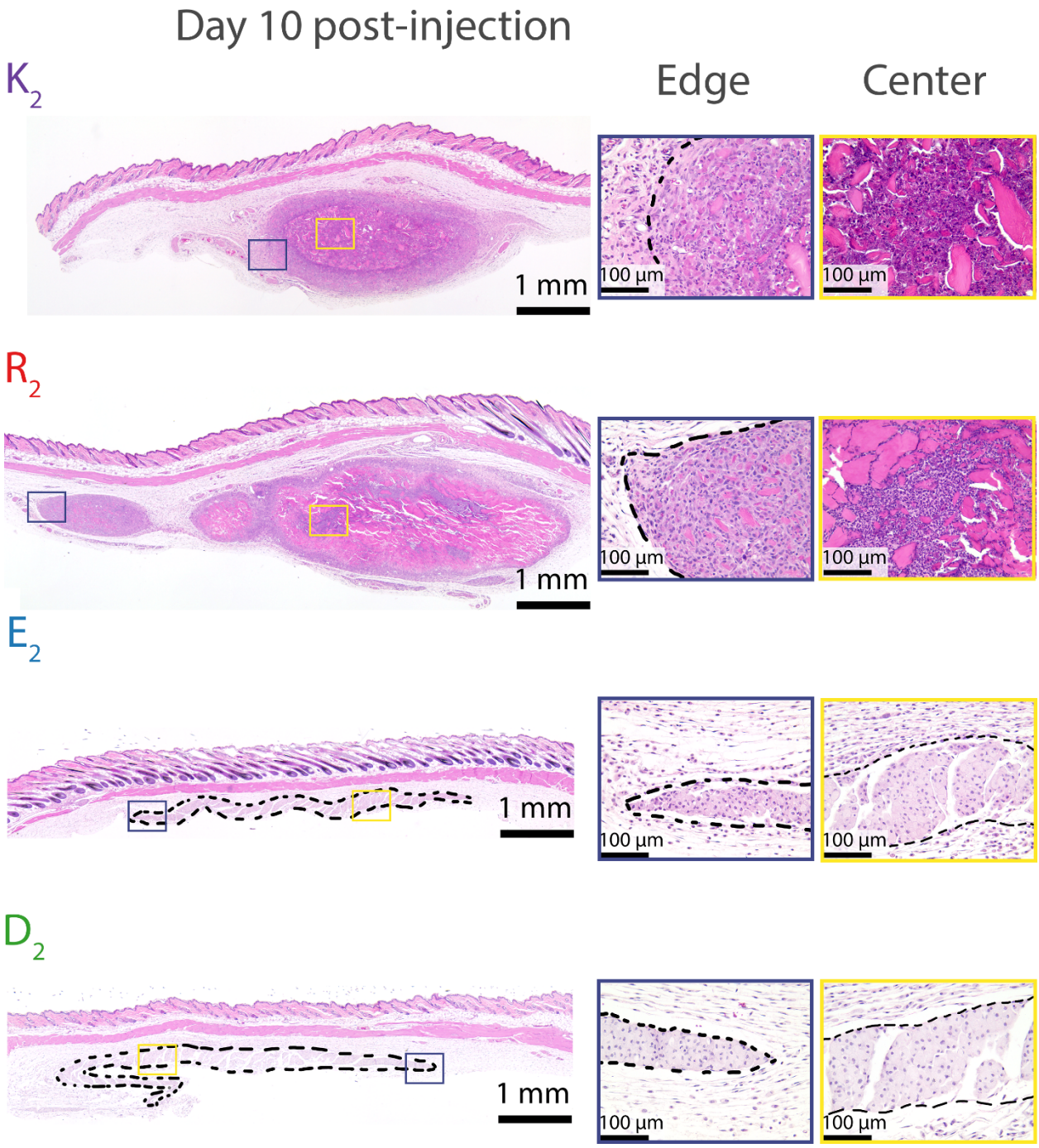

Figure S8. H&E staining of the whole implant of K_2. R_2, E_2, D_2 at day 10 post-injection. The purple box represents the area of the implant edge. The yellow box represents the area of the implant center. Dash lines represent the hydrogel in the subcutaneous space. Scale bar: 1 mm.

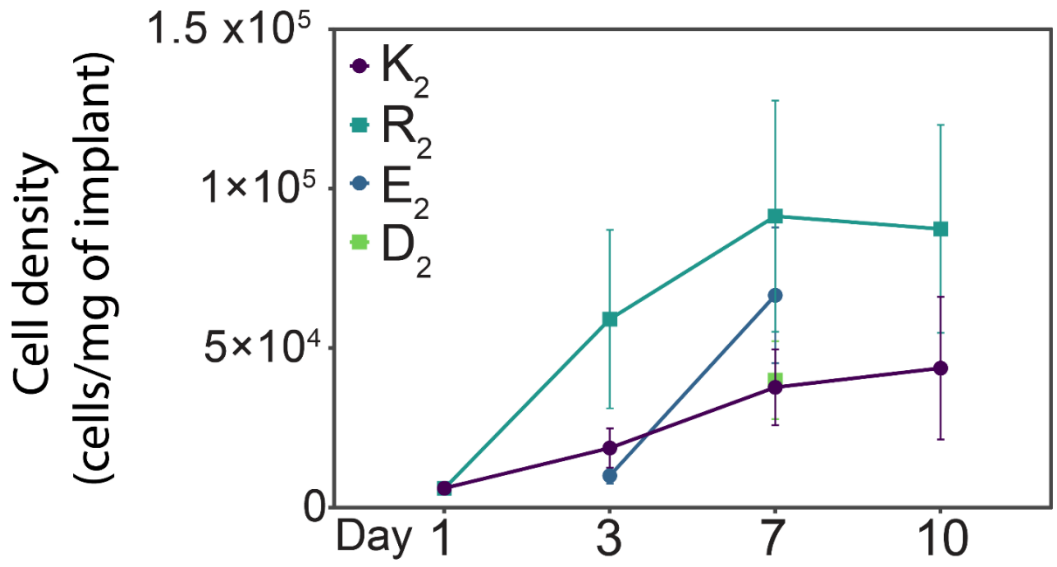

Figure S9. Cell density present in the MDP implants at different time points.

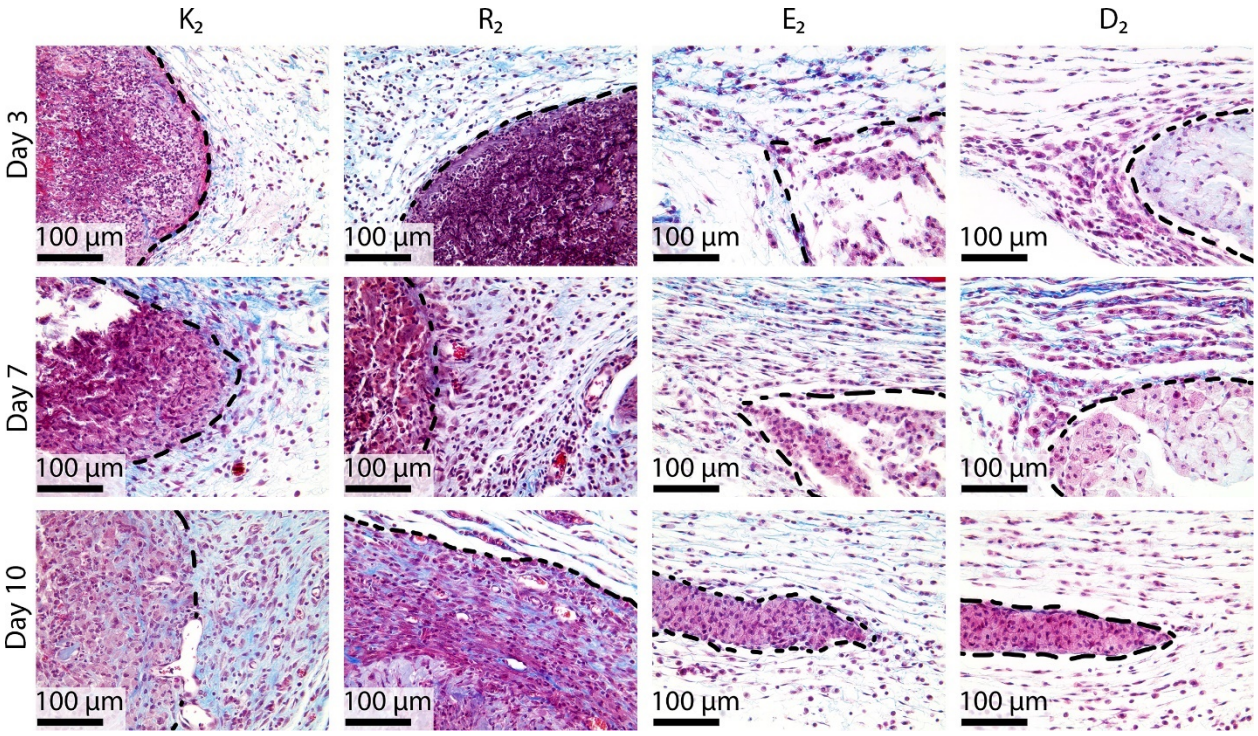

Figure S10. Collagen deposition and tissue remodeling of MDP hydrogel implants. Masson's Trichrome staining of implant cross-sections at day 3, 7 and 10 post-injection to observe collagen deposition in color blue. Images represent the interface between hydrogel and native tissue. By Day 10, K_2 and in particular R_2 show larger collagen deposition, whereas the negatively-charged MDPs have been degraded and remodeled into native tissue.

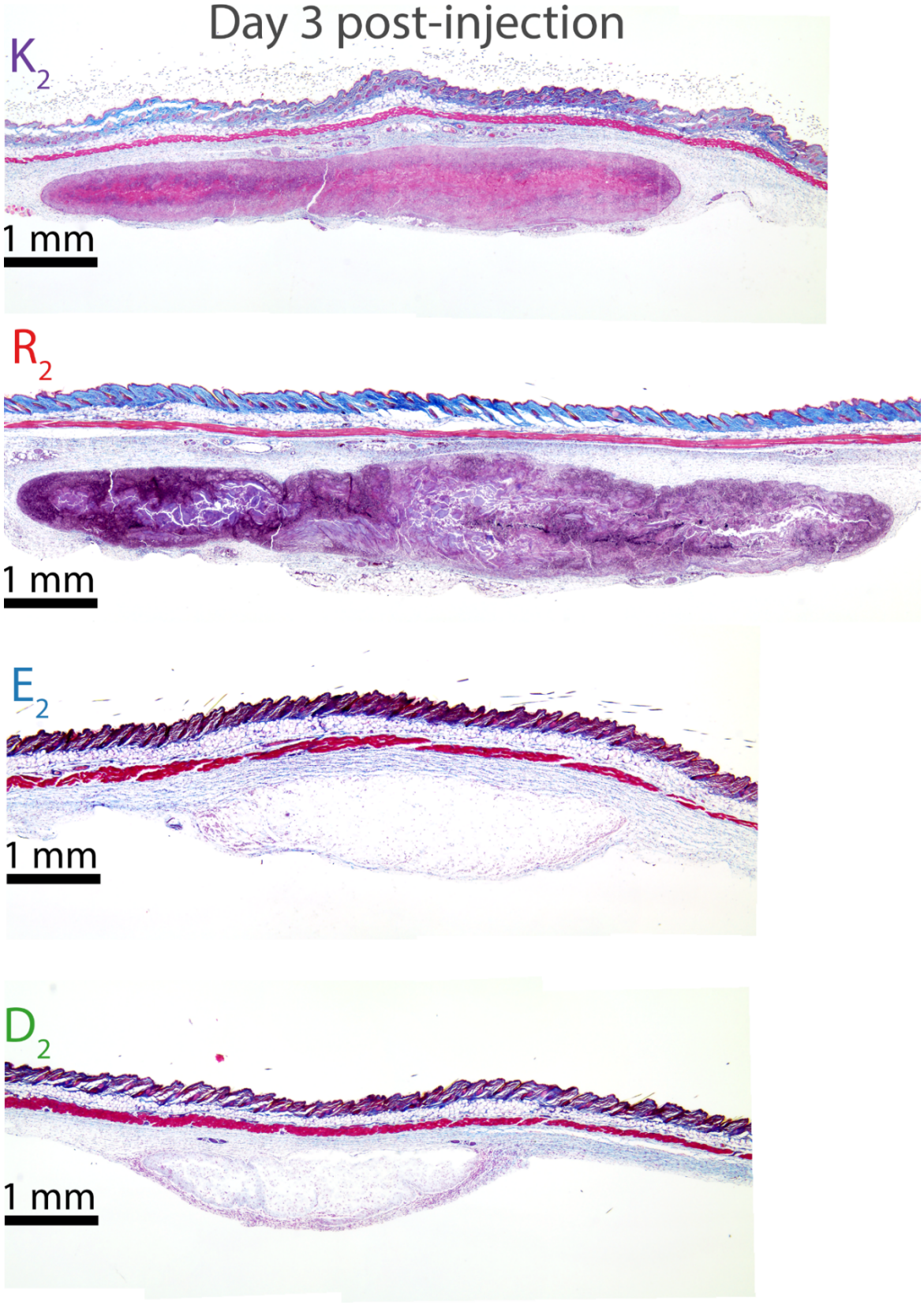

Figure S11. Masson's Trichrome staining of the whole implant of K_2. R_2, E_2, D_2 at day 3 post-injection. Scale bar: 1 mm.

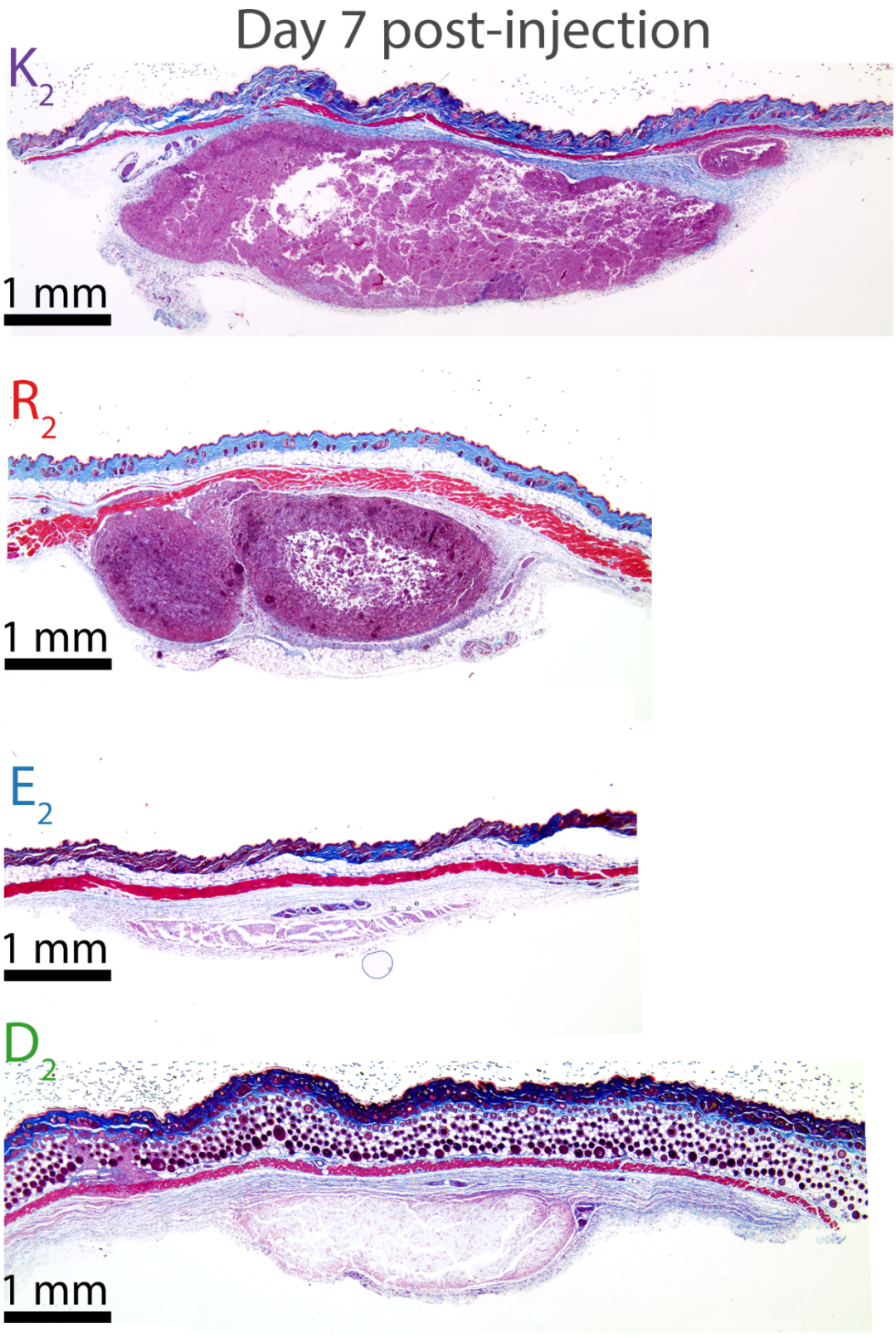

Figure S12. Masson's Trichrome staining of the whole implant of K_2. R_2, E_2, D_2 at day 7 post-injection. Scale bar: 1 mm.

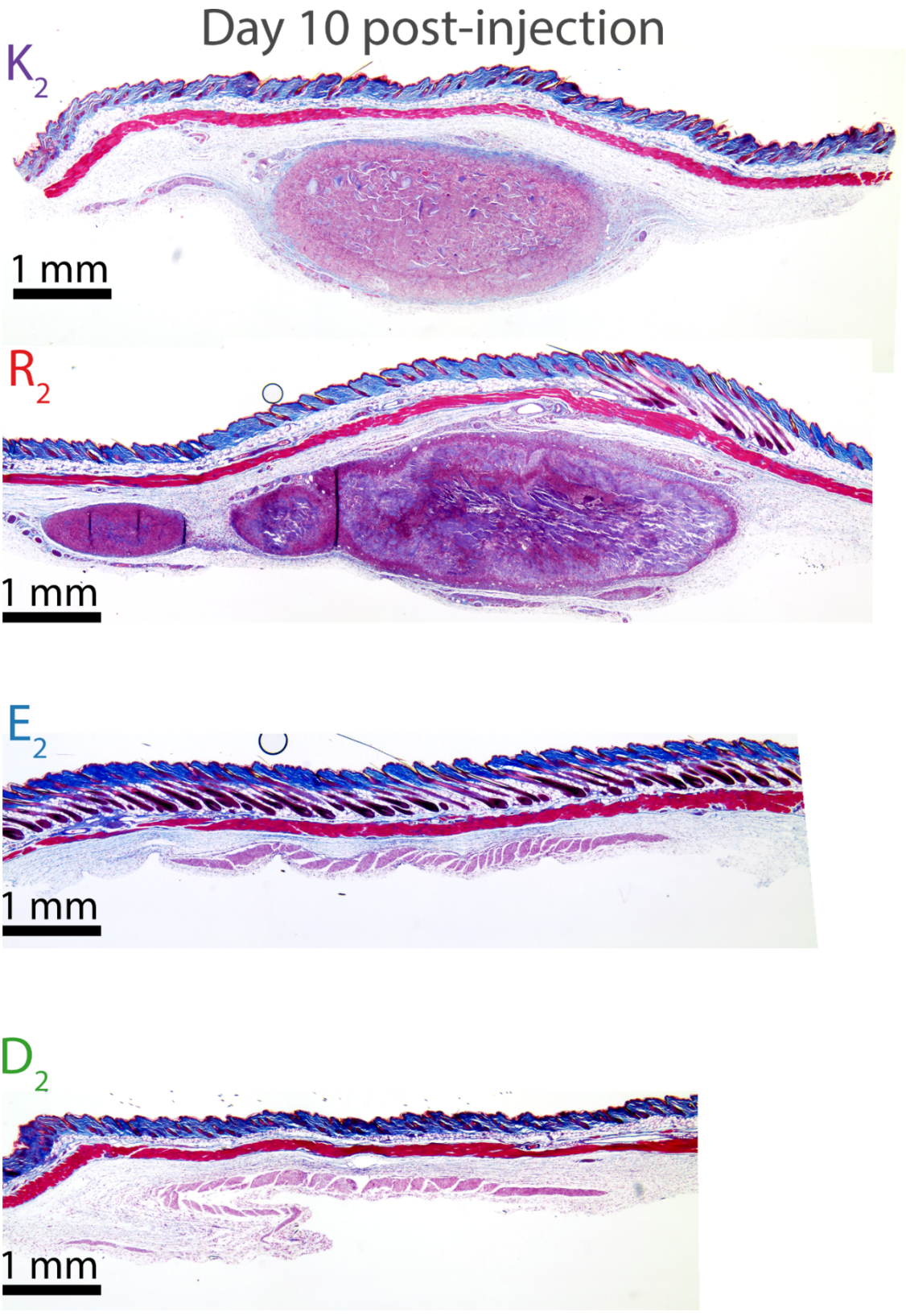

Figure S13. Masson's Trichrome staining of the whole implant of K_2. R_2, E_2, D_2 at day 10 post-injection. Scale bar: 1 mm.

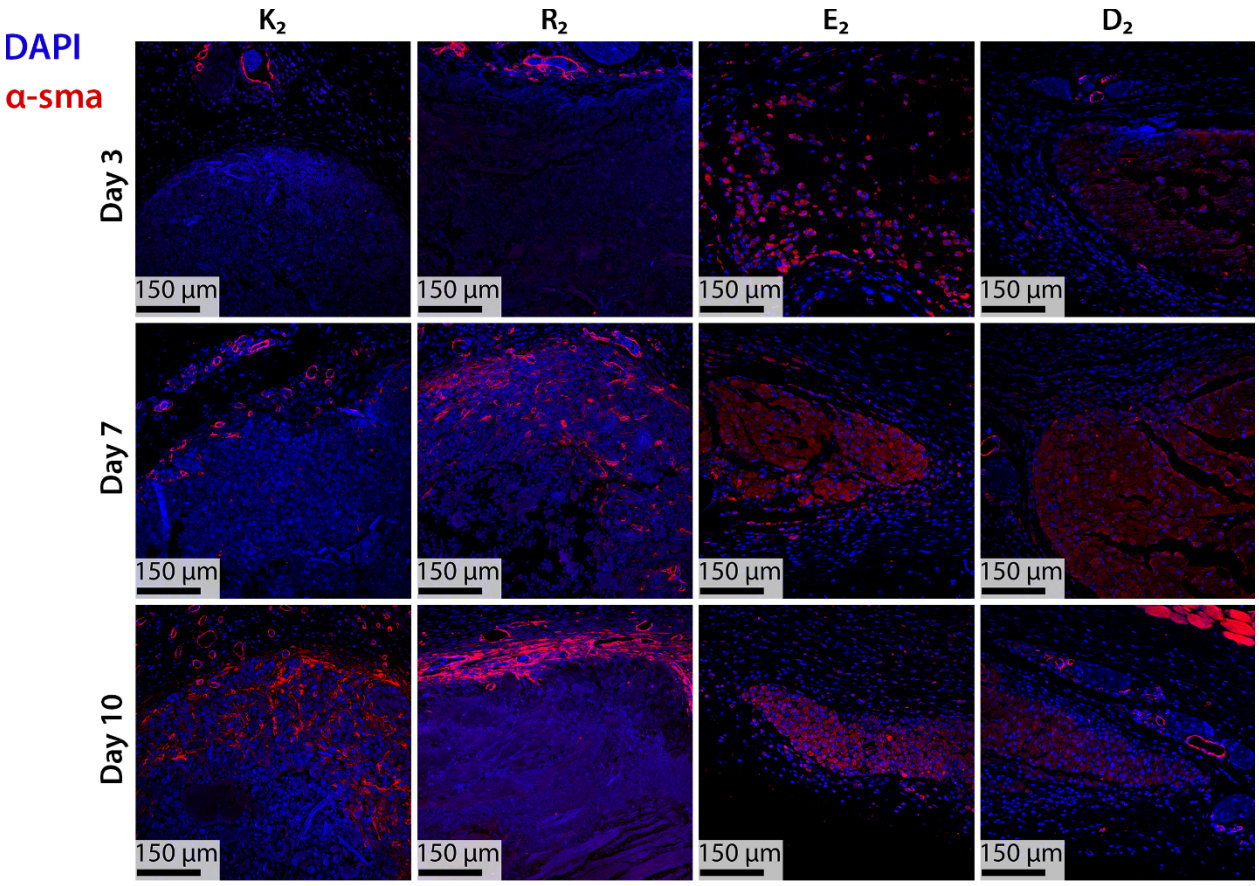

Figure S14. Immunostaining of alpha-smooth-muscle actin at the edge of the implants at day 3, 7 and 10 post-injection. Positive α -sma expression is shown in red and cell nuclei in blue (DAPI staining). Scale bar 150 μm.

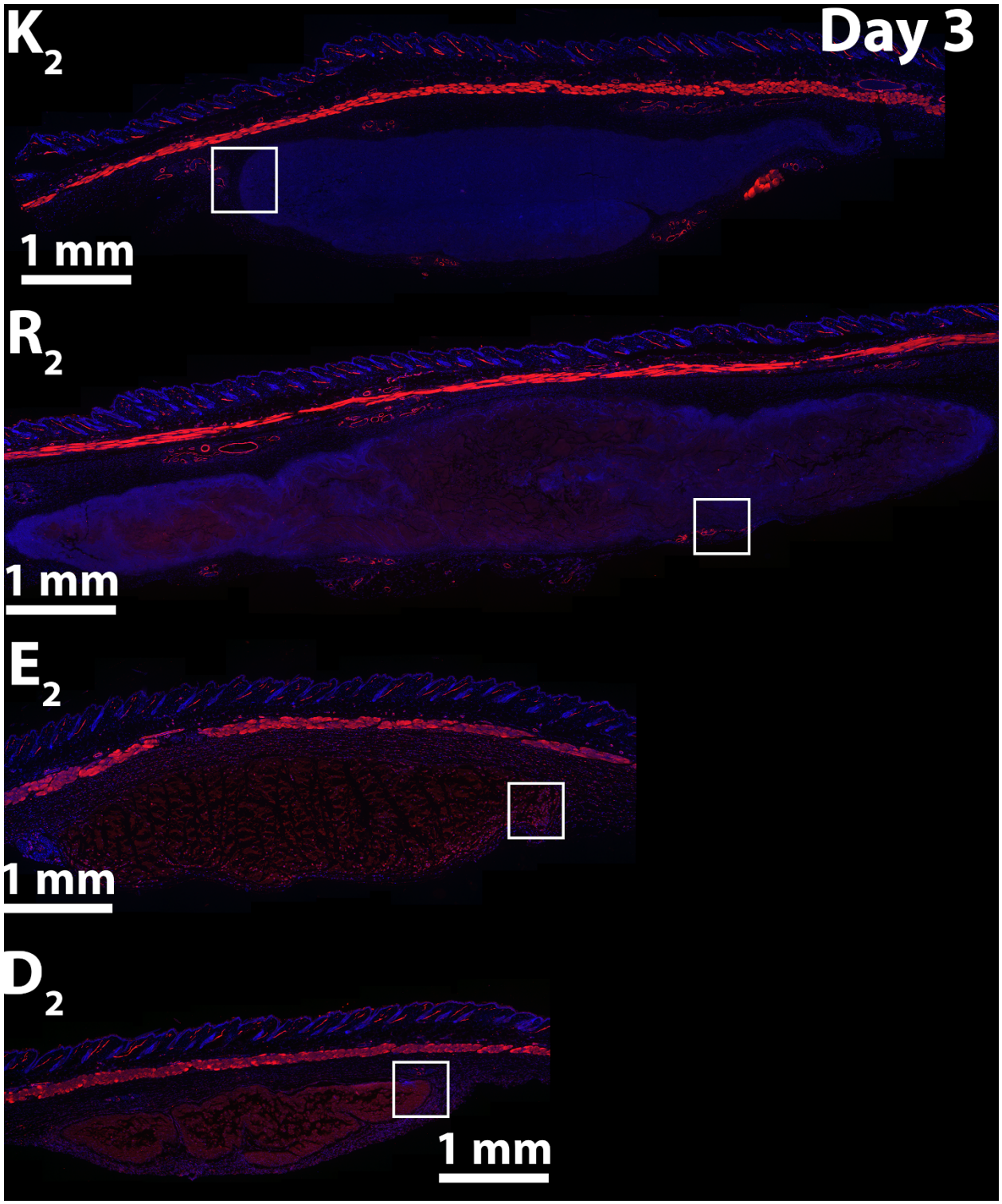

Figure S15. Immunostaining of alpha-smooth-muscle actin (red) and cell nuclei (blue) of the whole implant of K_2. R_2, E_2, D_2 at day 3 post-injection. Scale bar: 1 mm.

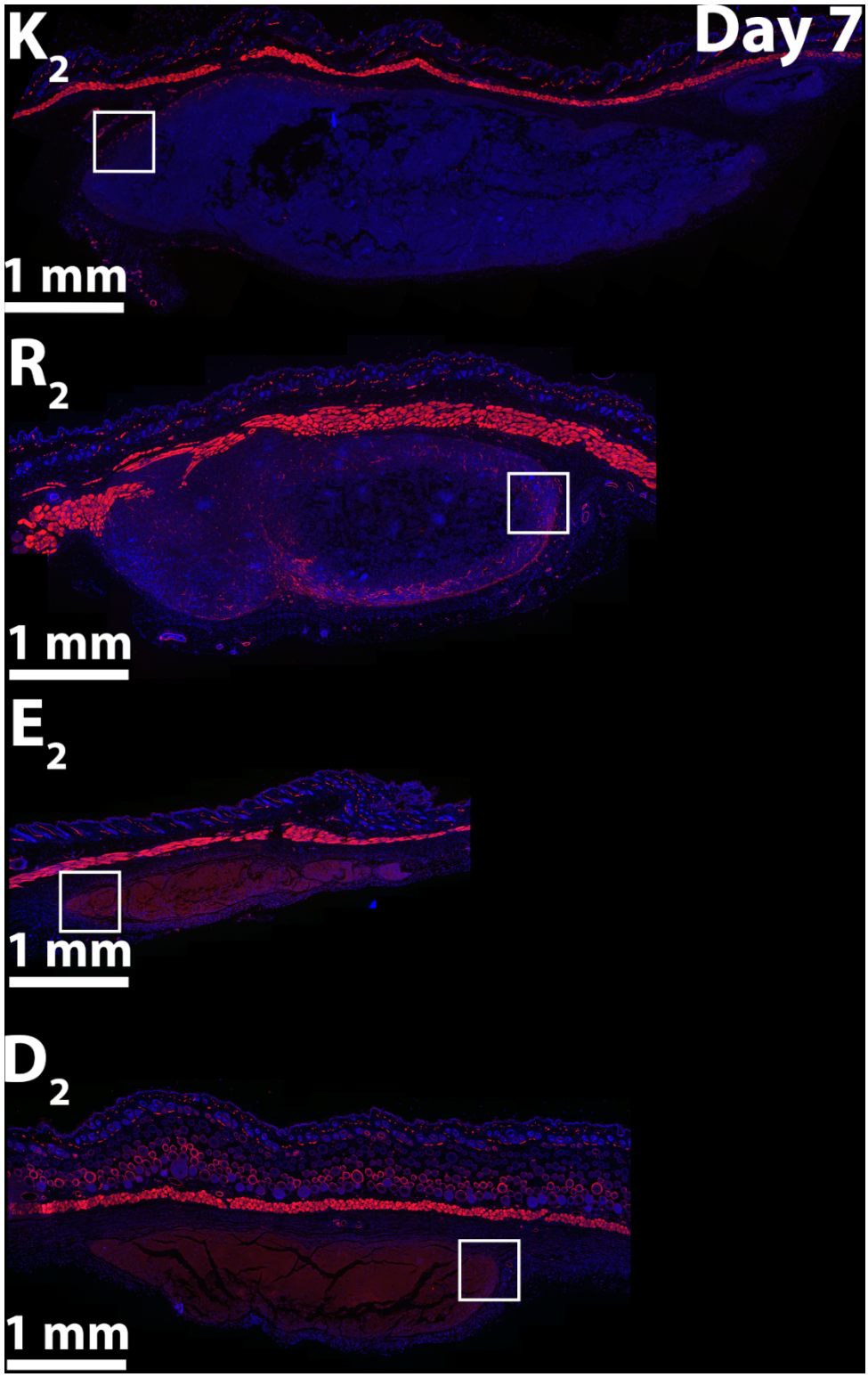

Figure S16. Immunostaining of alpha-smooth-muscle actin (red) and cell nuclei (blue) of the whole implant of K_2. R_2, E_2, D_2 at day 7 post-injection. Scale bar: 1 mm.

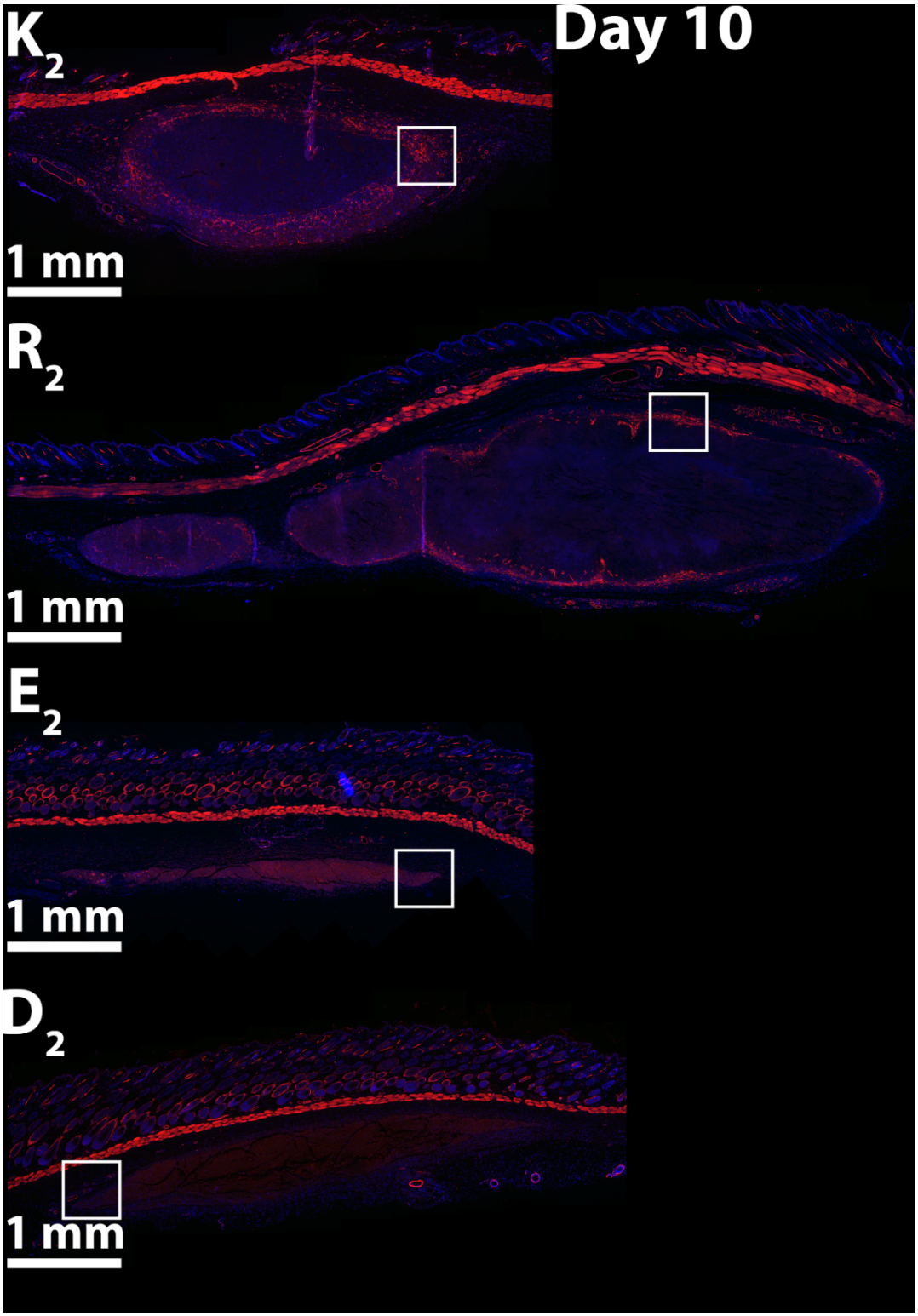

Figure S17. Immunostaining of alpha-smooth-muscle actin (red) and cell nuclei (blue) of the whole implant of K_2. R_2, E_2, D_2 at day 10 post-injection. Scale bar: 1 mm.

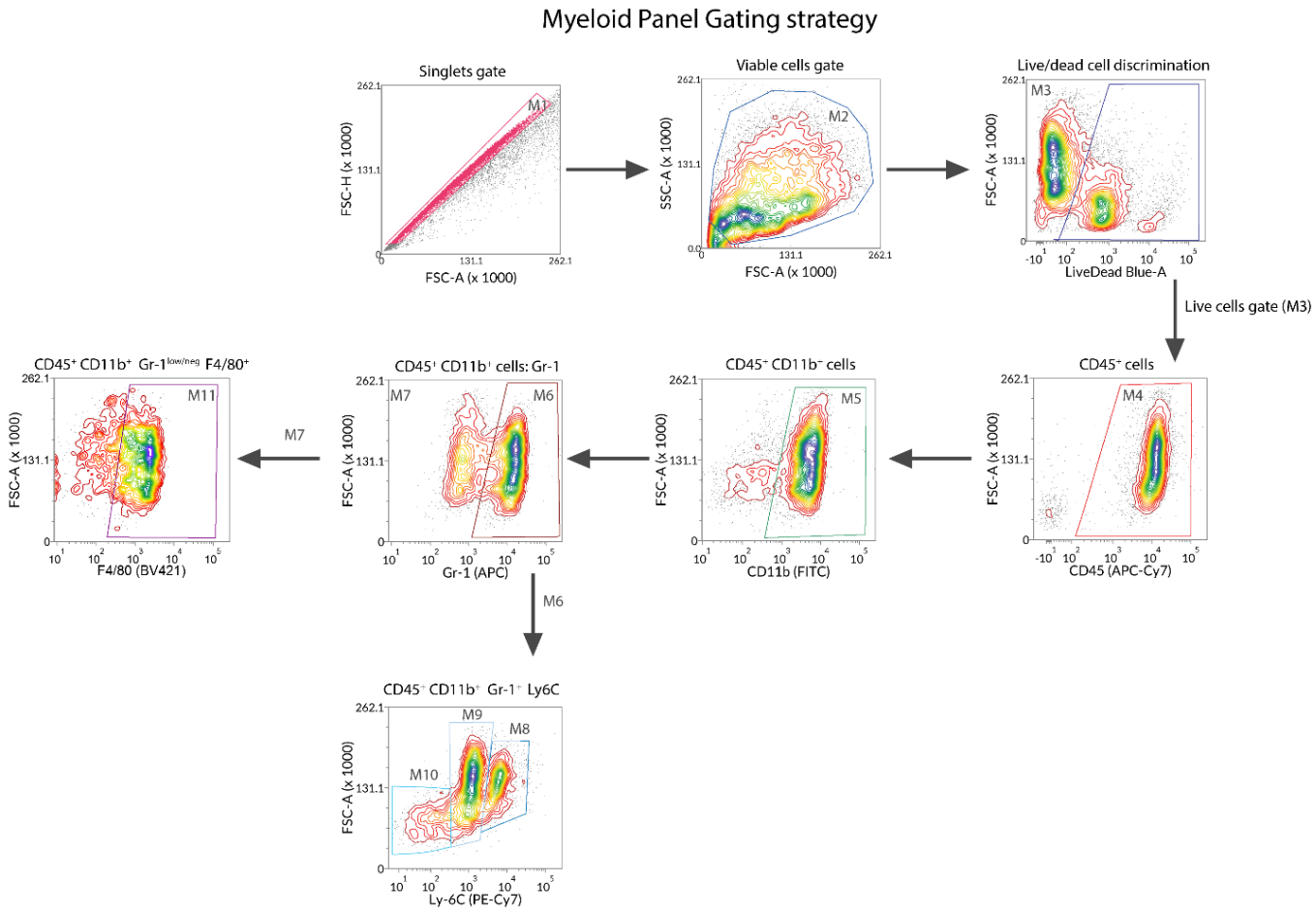

Figure S18. Gating strategy for the immunophenotyping of myeloid cells in the MDP hydrogels. M1 single cells after doubles discrimination (FSC-A vs FSC-H). M2 viable cells from M1. M3 Live cells after live/dead discrimination followed by immune CD45+ cell gating. Immune cells of myeloid origin (M5) were classified according to Gr-1, Ly6C and F4/80 expression (M6-M11).

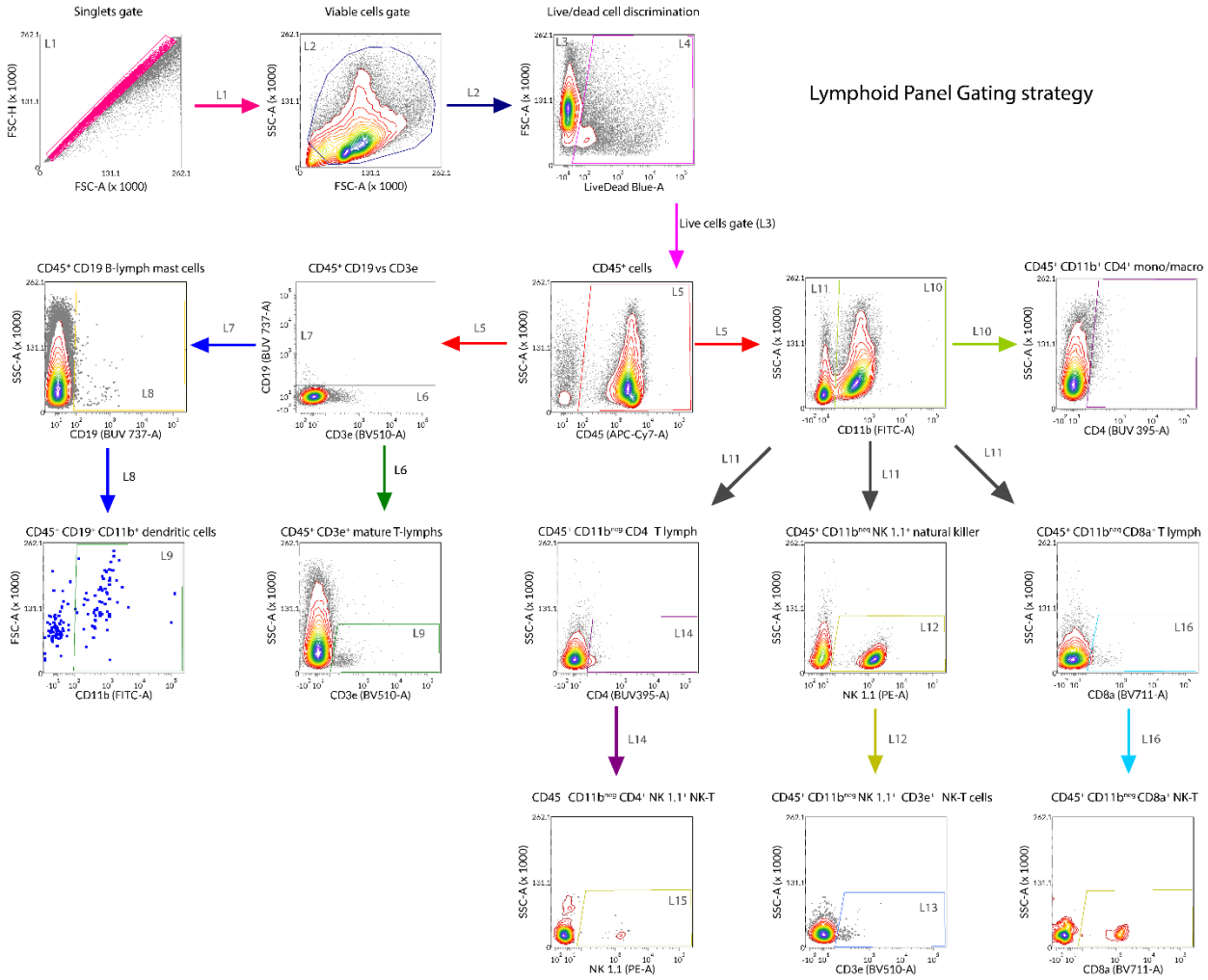

Figure S19. Gating strategy for the immunophenotyping of lymphoid cells in the MDP hydrogels.

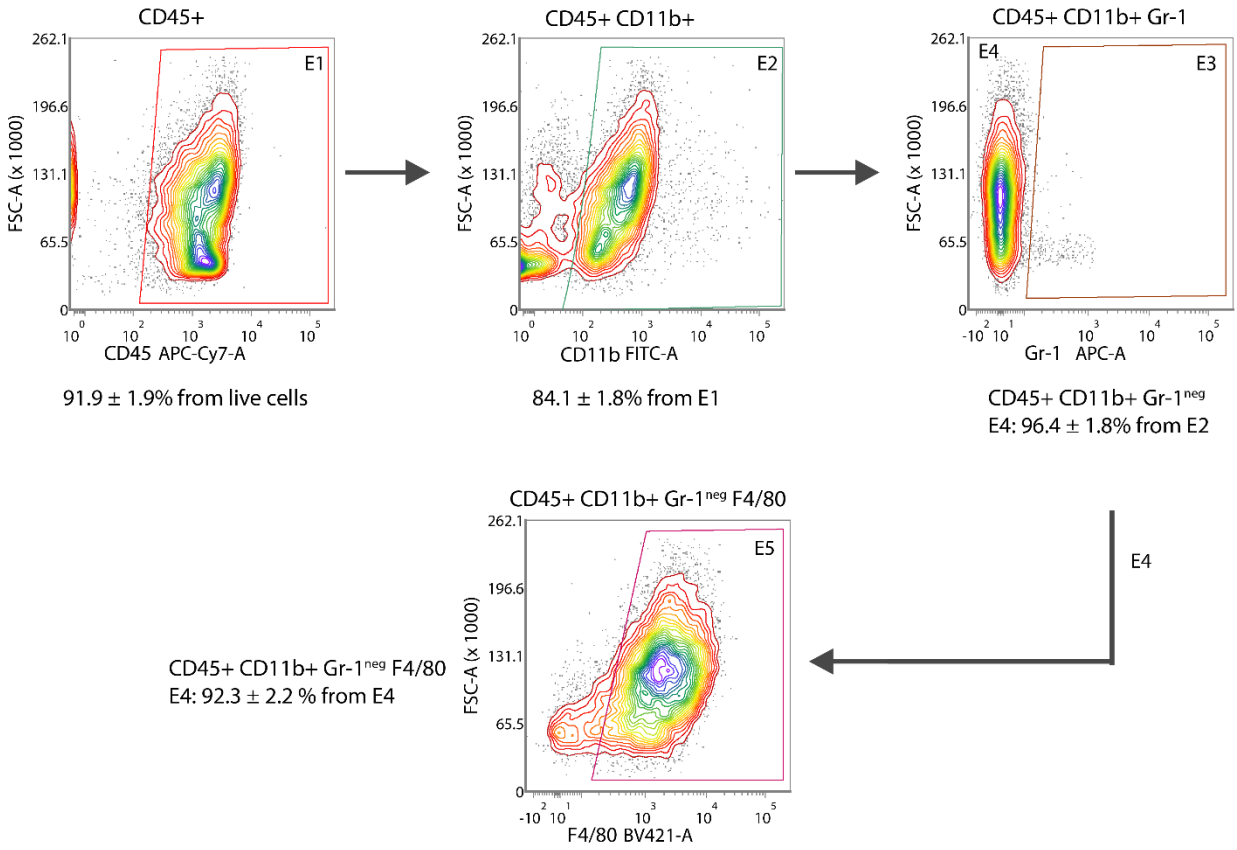

Figure S20. Immunophenotyping of infiltrating cells in E_2 implants at day 3.

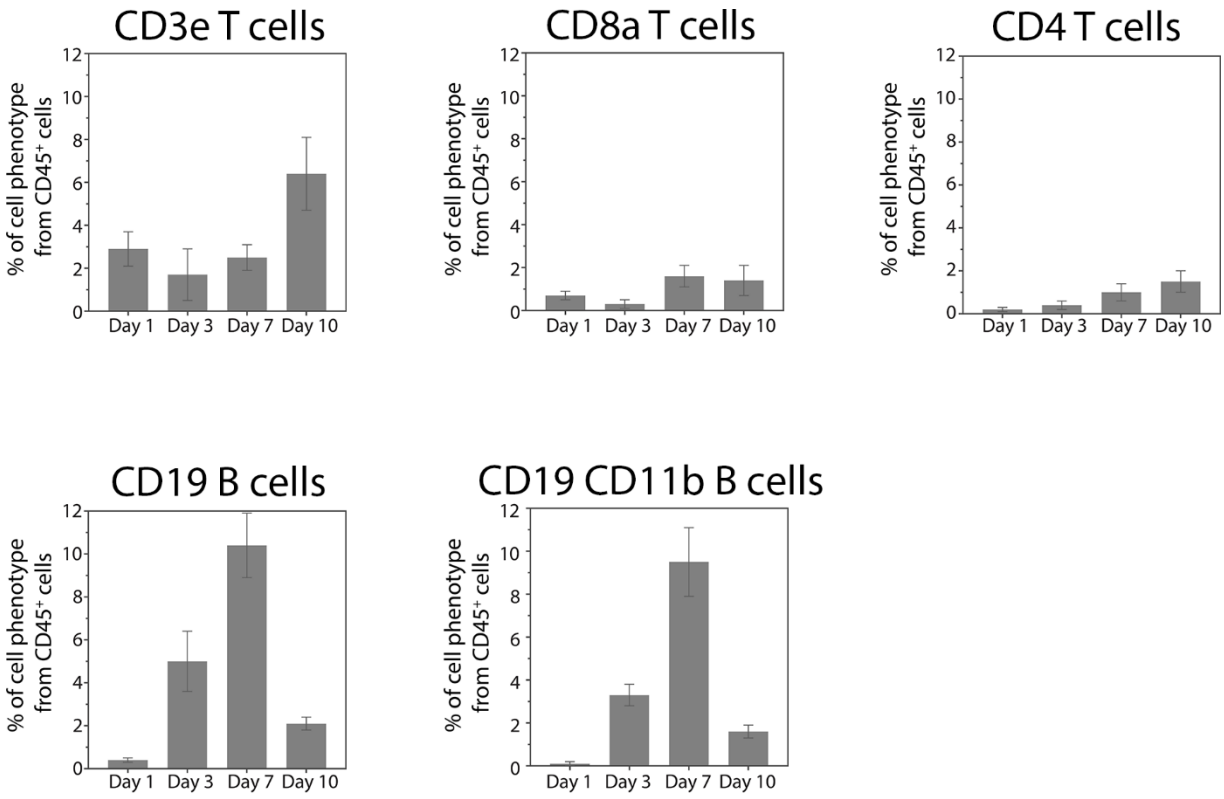

Figure S21. Percentage of different lymphoid cell phenotypes from CD45+ cells present in K_2 implants at day 1, 3, 7 and 10 post-injection.

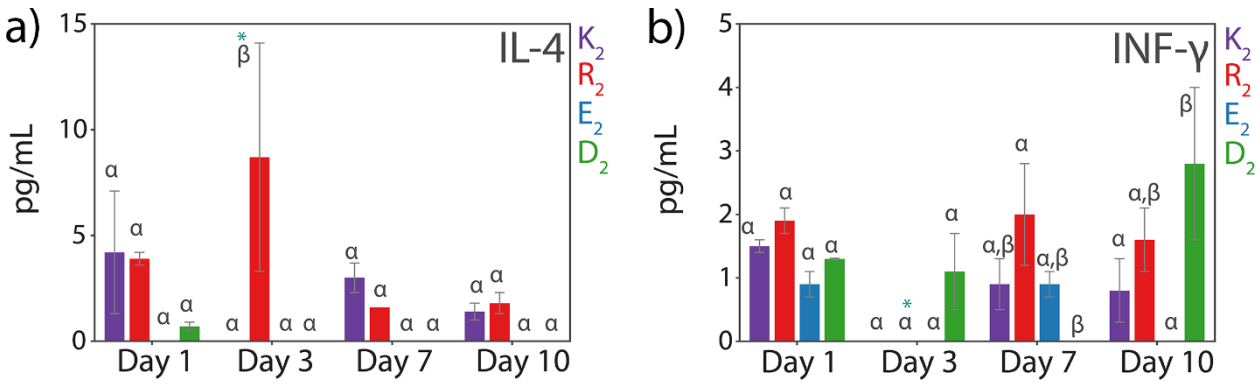

Figure S22. Quantification of IL-4 and INF-γ from the implant lysate.

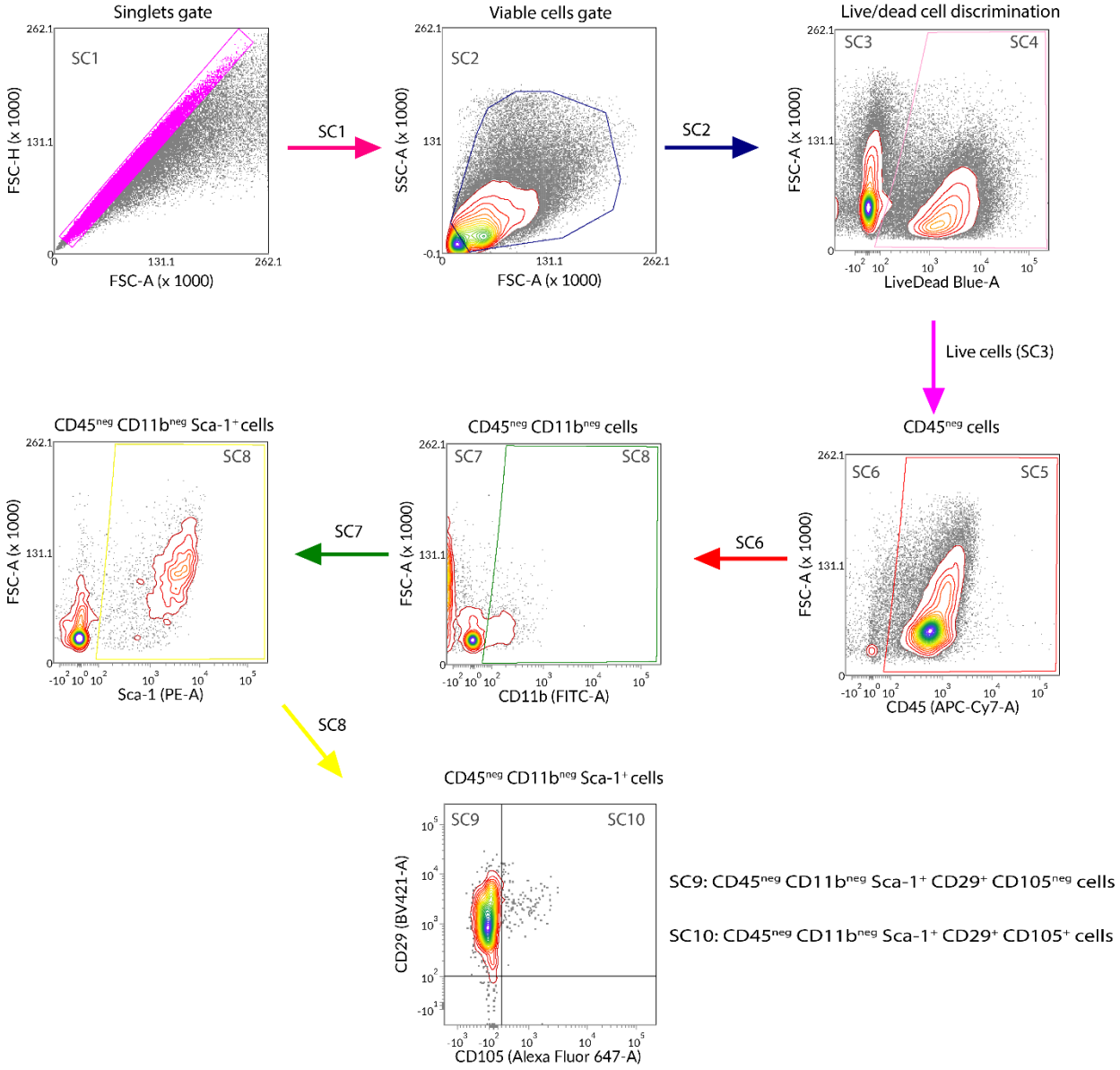

Figure S23. Gating strategy for the immunophenotyping of stem cells in the MDP hydrogels.